Physics Letters A 523 (2024) 129806

Contents lists available at ScienceDirect

Physics Letters A

journal homepage: www.elsevier.com/locate/pla

Letter

Sorting of dynamical crystallization from dynamical fermionization: A quantum many-body approach

Barnali Chakrabarti [a,c,*], Pankaj Kumar Debnath [b], Arnaldo Gammal [c]

[a] Department of Physics, Presidency University, 86/1 College Street, Kolkata 700073, West Bengal, India
[b] Swami Vivekananda High School (H.S.), Garshyamnagar-II, Shyamnagar, 24 Parganas (N), 743127, West Bengal, India
[c] Instituto de Física, Universidade de São Paulo, CEP 05508-090, São Paulo, Brazil

ARTICLE INFO

Communicated by B. Malomed

Keywords:
Quench dynamics
Fermionization
Crystallization

ABSTRACT

Dynamical fermionization refers to the phenomenon when the momentum distribution of impenetrable bosons asymptotically reaches that of non interacting fermions on sudden release from the trap. Whereas on sudden change in trap frequency results to Bose-Fermi oscillation which has been experimentally confirmed in the case of the Lieb-Liniger model in the Tonks-Girardeau (TG) regime. Crystallization happens for sufficiently strongly interacting repulsive bosons with dipolar interactions in one spatial dimension. Crystallization resembles fermionization but distinctly different due to long-range interaction. The present work aims to distinguish dynamical crystallization from dynamical fermionization in the expansion and breathing dynamics of $N = 4$ strongly interacting bosons in TG limit. Our results suggest that the N-fold complete splitting in one-body density for dipolar bosons makes a clear signature of crystallization in the Bose-Fermi oscillation. We investigate the many-body dynamics by employing multiconfigurational time-dependent Hartree method for bosons which solve the N-body time-dependent Schrödinger equation numerically exactly.

1. Introduction

The out-of-equilibrium dynamics of isolated strongly correlated many-body systems become one of the most challenging problems in quantum dynamics. The accurate time-dependent control of microscopic parameters for the ultracold trapped atomic gases offers a better understanding of the manipulation of many-particle quantum states and realization of non-equilibrium process [29,8,9]. One dimensional (1D) systems are the ideal test beds for the study of out-of-equilibrium dynamics due to strong interatomic correlations. In the reduced dimension, quantum effects are more important, and quantum fluctuations are also enhanced for strong interactions. The simplest way to study out-of equilibrium process is the quantum quench.

Observation of dynamical fermionization–when the physical properties of impenetrable bosons (Tonks-Girardeau gas) dynamically achieve the properties of noninteracting fermions, is the most seminal observation in this field. It was theoretically predicted for the bosonic Lieb Liniger model with infinite repulsion [16,20,19], on sudden release of the trap, the momentum distribution evolves from bosonic to fermionic character [15,25,30,26,40]. This prediction was experimentally observed in the recent experiments [39,18,14]. The 1D expansion is achieved by turning off the longitudinal confinement–the gas develops a Fermi shape of the momentum distribution. Whereas an abrupt change in the trap frequency induces large amplitude breathing oscillation–'Bose-Fermi' oscillation. Over the past few years, the study of "dynamical fermionization" has been extended for one-dimensional spinor quantum gases [2] and 1D Bose-Fermi mixture [27].

However, a more interesting observation is the crystallization which emerges for strongly interacting bosons with dipolar interaction in one spatial dimension. Dipolar ultracold atoms have attracted much interest which is corroborated by experimental realization of dipolar Bose Einstein condensate consists of chromium [17], dysprosium [24] and erbium atoms [1]. The long range dipole-dipole interaction and its anisotropic nature leads to rich and exotic many-body physics which are distinctly different from the Bose Einstein condensate (BEC) with contact interaction [10,12]. One such phenomenon is the crystallization in one- and two-dimensional system [4,43,42,6,5,13]. Crystallization is the consequence of strong repulsive long-ranged tail of the dipolar interaction when the bosons exhibit maximal separation. Crystallization resembles fermionization as in both cases bosons either minimize or

* Corresponding author.
E-mail addresses: barnali.physics@presiuniv.ac.in (B. Chakrabarti), pankaj_phys@yahoo.com (P.K. Debnath), gammal@if.usp.br (A. Gammal).

https://doi.org/10.1016/j.physleta.2024.129806
Received 18 April 2024; Received in revised form 13 August 2024; Accepted 14 August 2024
Available online 22 August 2024

escape spatial overlap due to strong interaction. However, unlike the fermionization with strong contact interaction, the energy of the crystallized bosons does not saturate (explained later). These two phases have already been established as two hallmark phases of strongly correlated one-dimensional bosonic systems [7]. As a consequence, the N-fold splitting in one-body density for the fermionized bosons is incomplete and restricted by the external trap. In contrast, the splitting is complete for dipolar bosons, due to the long-range tail in the dipolar interaction, the interaction energy can overcome the confining potential and exhibit very fast spreading upon quench.

In this article, we like to explore the out-of-equilibrium dynamics of strongly correlated dipolar bosons– termed as "dynamical crystallization" and compare them to the dynamical fermionization from a many-body perspective. Dynamical crystallization is an well established technique in the experiments [28,36], which provide the coherent control of the many-body systems. Rydberg atoms are the ideal test bed which exhibit unique properties, the strong van der Waals interaction can be manipulated to create many-body phases in neutral ultracold atom samples. The dynamic process of crystallization in the transverse field of Ising model has also recently been explored [41].

We prepare the initial state at the ground state of a few interacting bosons in a harmonic oscillator potential. We make the system trapless by the sudden removal of the trap and explore the signature of crystallization in the dynamical phases of the many-body wave function. We also initiate the breathing oscillation on sudden reduction of trap frequency and observe very rich dynamical evolution in momentum space. The usual Bose-Fermi like oscillation and frequency doubling are observed in both dynamical crystallization and dynamical fermionization. However, the repulsive long-range tail of the dipolar interaction dominates the crystallization process–maximally separated bosons are identified in the entire dynamics. The N-fold splitting in the one-body density unequivocally identifies the dynamical crystallization and distinguishes it from the dynamical fermionization. The dynamics for one-body correlation nicely present how the crystallization happens. We additionally present the spreading of density and dynamical fragmentation to distinguish the two dynamical processes.

We solve the N-body time-dependent Schrödinger equation numerically with very high precision using the multiconfigurational time-dependent Hartree for bosons (MCTDHB) which calculates the many-body wave function numerically exactly [3,38,22,21,23]. The key measures are one-body densities in real and momentum space and Glauber correlation function.

2. Hamiltonian and set up

The time-dependent Schrödinger equation for N interacting bosons is given by

$$H|\psi(t)\rangle = i\frac{\partial}{\partial t}|\psi(t)\rangle \tag{1}$$

We use dimensionless unit defined by dividing the Hamiltonian by $\frac{\hbar^2}{mL^2}$, m is the mass of a boson, L is the length scale. H is the N-particle Hamiltonian

$$H = \sum_{i=1}^{N} h(x_i) + \sum_{i<j} W(x_i - x_j) \tag{2}$$

where $h(x_i) = -\frac{1}{2}\frac{\partial^2}{\partial x_i^2} + V(x_i)$ is the one-body Hamiltonian. $V(x_i) = \frac{1}{2}\omega_0 x_i^2$ is the external harmonic trap. $W(x-x')$ is the two-body interaction. For contact interaction $W(x-x') = \lambda\delta(x-x')$, λ is the interaction strength and is determined by the scattering length and the transverse confinement. The quasi-1D regime is ensured by strong transversal confinement which provides a cigar-shaped density of atoms. For dipolar interaction $W(x-x') = \frac{g_d}{|x-x'|^3+\alpha_0}$, g_d is the pure dipolar interaction strength; $g_d = \frac{d_m^2}{4\pi\epsilon_0}$ for electric dipoles and $g_d = \frac{d_m^2\mu_0}{4\pi}$ for magnetic dipoles, d_m being the dipole moment, ϵ_0 is the vacuum permittivity, and μ_0 is the vacuum permeability. α_0 is the short-range cutoff to avoid singularity at $x = x'$. We choose $\alpha_0 = 0.05$ and check the consistency when the dipolar interaction is augmented with a contact potential. Choice of $\alpha_0 = 0.05$ also corresponds to $a_\perp = 0.37$ and an aspect ratio $= 42.5$ [37,13]. In general, the dipole-dipole interaction potential in 1D also includes a contact term owing to the transverse confinement, however that can be safely neglected for strong interaction strengths [11]. We focus on $N = 4$ interacting bosons and consider two specific cases of strongly interacting limit $\lambda = 25$ and $g_d = 25$.

3. Numerical method

In MCTDHB, the many-body wave function $|\psi(t)\rangle$ of N interacting bosons is expanded as the linear combination of time-dependent permanents [3,38,33,32]

$$|\psi(t)\rangle = \sum_{\vec{n}} C_{\vec{n}}(t)|\vec{n};t\rangle. \tag{3}$$

The time-dependent permanents $\{|\vec{n};t\rangle\}$ are obtained by distributing N bosons over M time-dependent orbitals $\{\phi_i(x,t)\}$. The permanents are symmetrized bosonic many-body states and are referred to as "configurations". The vector $\vec{n} = (n_1, n_2, \ldots, n_M)$ represents the occupation of the orbitals and $n_1 + n_2 + \cdots + n_M = N$ preserves the total number of particles. The sum in Eq. (3) runs over all configurations of N particles distributed in M orbitals. Eq. (3) spans the full N-body Hilbert space in the limit of $M \to \infty$. Thus MCTDHB is exact by its construction. However, for practical computations, we restrict to the number of orbitals and convergence in several measures like the one- and two-body density matrix, which determines the required number of orbitals.

The expansion coefficients $\{C_{\vec{n}}(t)\}$ and the orbitals $\{\phi_i(x,t)\}$, both are time-dependent and are determined by the time-dependent variational principle. A set of coupled equations of motions for $\{C_{\vec{n}}(t)\}$ and $\{\phi_i(x,t)\}$ are obtained by requiring the stationarity of the action of the time-dependent Schrödinger equation concerning the variations of the expansion coefficients and the orbitals [21,34,31]. MCTDHB is fundamentally different from exact diagonalization which uses the time-independent orbitals as the many-body ansatz. We stress here that MCTDHB delivers solutions of the Schrödinger equation with much more accuracy than exact diagonalization methods at the same dimensionality of the considered space. As in exact diagonalization, the time-independent basis built from the eigenstates of a one-body problem, are not further optimized to take into account the dynamics and correlations in the considered system, which necessarily arise due to the presence of interparticle correlation. In this sense, the Hilbert space and basis used in exact diagonalization are fixed and not optimized.

We solve the set of coupled MCTDHB equations implemented in the MCTDH-X software [23]. For the present computation of $N = 4$ strongly interacting bosons in TG limit, the convergence is established in the key measures with orbital $M = 24$.

4. Quantity of interest

From the time-dependent wave function, the reduced one-body density matrix is defined as

$$\rho^{(1)}(x|x';t) = \langle\psi(t)|\hat{\psi}^\dagger(x')\hat{\psi}(x)|\psi(t)\rangle \tag{4}$$

where $\hat{\psi}(x)$ is the bosonic field operator which annihilates a particle at the position x. The diagonal part of the one-body density matrix,

$$\rho(x;t) = \rho^{(1)}(x|x'=x;t) \tag{5}$$

is the usual one-particle density at time t which probes the spatial distribution of the bosons in the post quench dynamics.

To calculate the reduced one-body density matrix in momentum space one needs to follow Ref. [35]. It is defined as

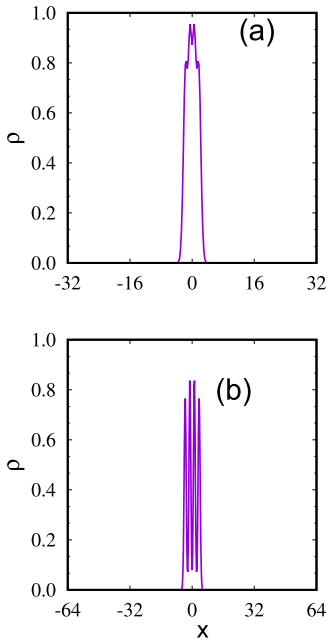

Fig. 1. One-body density of $N = 4$ strongly interacting bosons trapped in a harmonic oscillator potential of frequency $\omega_0 = 1.0$, for contact interaction of strength $\lambda = 25$ (a) and for dipolar interaction of strength $g_d = 25$ (b). In Fig. (a), four distinct but non isolated peaks mimic the density of four non interacting fermions. In Fig. (b), four fold splitting exhibits the crystal phase. Computation is done with $M = 24$ orbitals. All quantities are dimensionless.

$$\rho^{(1)}(k|k';t) = \langle \psi(t)|\hat{\psi}^{\dagger}(k')\hat{\psi}(k)|\psi(t)\rangle \tag{6}$$

and the diagonal part of it

$$\rho(k;t) = \rho^{(1)}(k|k' = k;t) \tag{7}$$

calculates the one-particle momentum distribution at time t. Thus, we investigate the dynamics by measuring two key quantities: real space, or x-space density dynamics, and momentum, or k-space density dynamics. To measure the degree of coherence we calculate the one-body Glauber correlation function

$$g^{(1)}(x,x';t) = \frac{\rho^{(1)}(x,x';t)}{\sqrt{\rho(x,t)\rho(x',t)}} \tag{8}$$

5. Results

5.1. Initial state

We perform the calculation for $N = 4$ repulsive interacting bosons trapped in the harmonic oscillator potential with $\omega_0 = 1.0$. We do the numerical simulation in the domain of $x_{min} = -32$ to $x_{max} = +32$ for contact interaction, whereas to accommodate the effect of long-range tail of the dipolar interaction we do the calculation in the range of $[-64, +64]$ and fix the number of orbitals to $M = 24$ which assure convergence of the fermionized and crystallized state in the parabolic trap. To investigate the stationary property we propagate the wave function in imaginary time using MCTDH-X software to solve the MCTDHB equations of motion, the system relaxes to the ground state. In Fig. 1(a), we plot the one-body density for the fermionized state with $\lambda = 25$ whereas Fig. 1(b) corresponds to the crystal state with $g_d = 25$. Fig. 1 discusses the similarity and contrast of these two states from a many-body perspective. The emergence of four maxima, which corresponds to the number of bosons in the trap, both for the contact and dipolar interaction confirms that the Tonks-Girardeau (TG) regime is achieved. However, the density modulations in the crystal state are significantly different compared to the fermionized state. For contact interaction, the density-maxima are

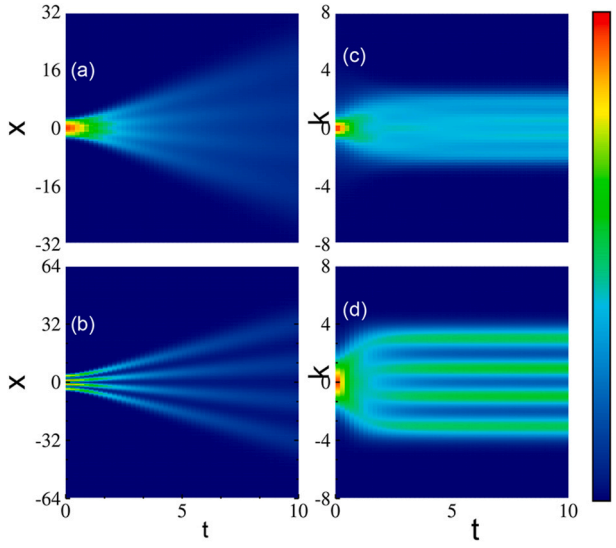

Fig. 2. The figure showcases the captivating time evolution of the density profile during the expansion of four strongly interacting bosons initially trapped in a harmonic oscillator (HO) potential and suddenly released. Fig. (a) and (b) correspond to density dynamics in x-space for contact interaction ($\lambda = 25$) and dipolar interaction ($g_d = 25$). Computations are done with orbital $M = 24$. Fig. (c) and (d) correspond to density dynamics in k-space for contact and dipolar interaction. See the text for details. All quantities are dimensionless.

not isolated due to binding nature of energy for contact interaction (explained later). The density modulation is maximum at the center of the trap where the potential is zero. Whereas the outermost humps are less modulated due to the larger distance from the center of the trap. However, for bosons with dipolar interaction in Fig. 1(b), the maxima are *well separated* due to the long-range tail of the interaction. In contrast with the fermionized state with contact interaction, for crystallized dipolar bosons, the value of the density at the minima between the humps tends to zero and the spreading of the density profile is broadened. Thus crystallization occurs due to the long-range tail of dipole-dipole interaction, the bosons form a lattice structure which allows them to minimize their mutual overlap.

5.2. Expansion dynamics of fermionized and crystallized bosons

To study the expansion dynamics of the bosons from fermionized and crystal states, we suddenly remove the trap and allow the bosons to expand. In Fig. 2(a) and (b) we plot the dynamics of one-body real space density for contact and dipolar interaction respectively. The clear many-body features are revealed in the dynamics, both for contact and dipolar interaction, as four bosons move independently as four bright jets. However, the density dynamics is distinctly different of the two states, both for short-time and long-time dynamics. Initially at time $t = 0$, bosons with contact interaction (Fig. 1(a)) are in a more confined position than the bosons with dipolar interaction (Fig. 1(b)). On expansion, four fermionized bosons cannot be distinguished clearly till time $t = 2.0$, after that, density exhibits four closed, confined peaks that further travel ballistically, independent of each other. Whereas the bosons with dipolar interaction (Fig. 1(b)), exhibit four completely isolated positions of four bosons initially at $t = 0.0$, which move further as four distinct bright jets independently. However, as a consequence of the repulsive long-range tail of the dipolar interaction, they spread very fast. It is to be noted that the spreading for contact interaction is observed in the much smaller domain. We further suggest that the very fast spreading for dipolar bosons is the consequence of rapid growth in energy which is in stark contrast for contact interaction as discussed later.

In Figs. 2(c) and (d), we plot the one-body density in momentum space for contact and dipolar interaction respectively. For contact in-

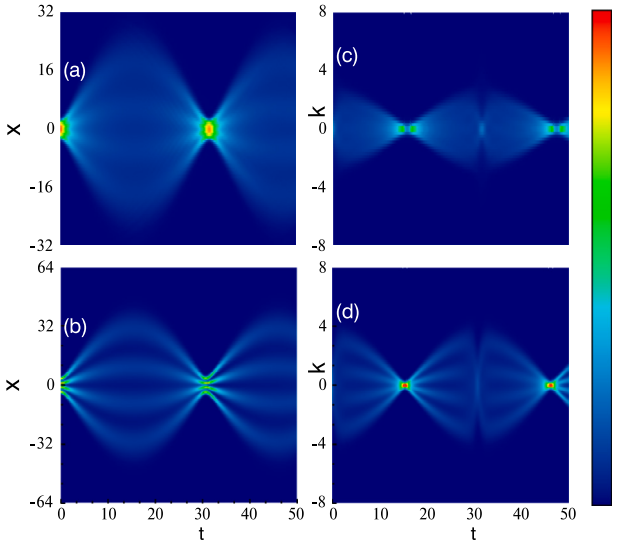

Fig. 3. The figure showcases the captivating dynamics after confinement quench from $\omega_0 = 1.0$ to $\omega_1 = 0.1$. Computations are done with orbital $M = 24$. Fig. (a) and (c) correspond to the real space and momentum space breathing dynamics for fermionized bosons. It clearly exhibits that periodic narrowing in momentum space occurs at twice of the density oscillation. Corresponding breathing dynamics for crystallized bosons are presented in Fig. (b) and (d) for the real space and momentum space. Due to strong diverging nature of dipolar interaction Fig. (b) exhibits regular dynamics only in the first half cycle before it is being destroyed. Frequency doubling in momentum space is observed in Fig. (d) only in the first cycle before it is being destructed. All quantities are dimensionless.

teraction (Fig. 2(c)), the one-body k-density is localized at the center. Then it splits into four–which expand further, and the width in momentum spreading is well converged. However, the two innermost jets are brighter than the two outermost jets. It is in close agreement with the observation made in Fig. 1(a), density modulation for fermionized bosons is not uniform, the innermost humps were stronger whereas the outermost humps were weaker. At $t = 8.0$, four peaks become stabilized and the density becomes exactly the same for four noninteracting fermions. Thus $t = 8.0$, is the time for dynamical fermionization. Fig. 2(d) for dipolar interaction, exhibits a clear signature of long-range tail in the dipole-dipole interaction. The one-body momentum density is completely fourfold and of equal intensity. It justifies Fig. 1(b), where the crystal state was diagnosed as four completely isolated peaks. However, in comparison with Fig. 2(c) for contact interaction, the width of momentum distribution for dipolar interaction is significantly larger in the entire dynamics.

5.3. Breathing oscillation of fermionized and crystallized bosons

A sudden change in the trap frequency to a nonzero value induces the so called breathing oscillation to the system. In the conventional experimental set up, few hundreds of atoms are trapped in quasi 1D scenario. The breathing mode is excited by quenching the axial confinement from ω_0 to ω_1 ($\frac{\omega_0}{\omega_1} > 1$). The resulting cloud evolves over time and the absorption image provided the density profile in the real and momentum space. The momentum distribution oscillates between the Fermi like and Bose like.

In our present computation, we reduce the frequency to one tenth of the initial frequency; $\omega_0 = 1.0$ to $\omega_1 = 0.1$. The results for ferminized bosons are presented in Fig. 3(a) and (c). The real space density [Fig. 3(a)] exhibits the self similar breathing cycle without any damping. While Fig. 3(c) represents the rich structure of bosonic-fermionic oscillation in the momentum space. The cloud is Bose like when it is broadest and Fermi like when it is the narrowest. The momentum distribution width becomes minimum when the real space density is the

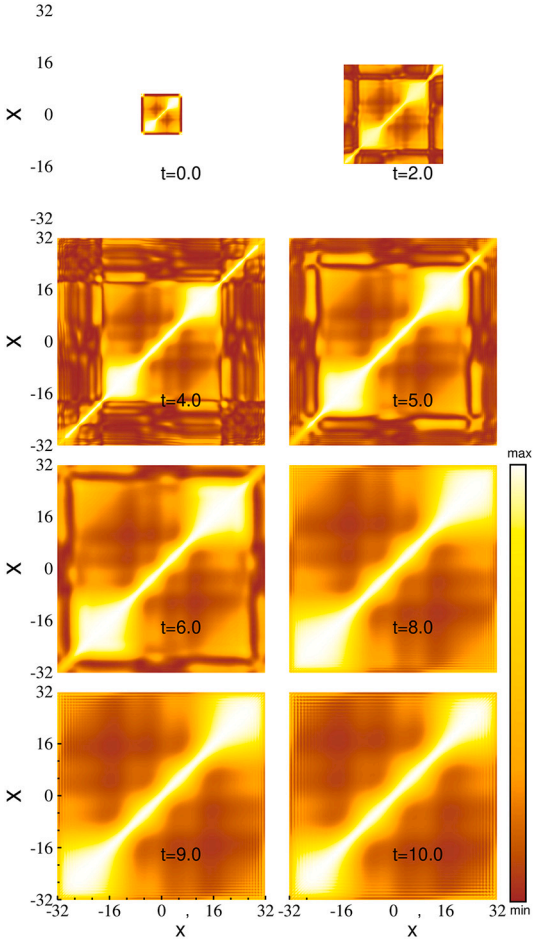

Fig. 4. Dynamics of one-body Glauber correlation function $g^{(1)}(x, x')$ for some selected times on sudden removal of the trap which initially confine four strongly interacting bosons with contact interaction in the Tonks-Girardeau limit. All quantities are in dimensionless unit.

broadest and the narrowest. The breathing dynamics also exhibit that the breathing frequency in real space is exactly double to the frequency in momentum space.

The corresponding breathing dynamics for crystallized bosons is presented in Fig. 3(b) and (d). The cloud with dipolar bosons again exhibit Bose-Fermi oscillation in the same time scale but rich structure is observed due to long-range tail of dipolar interaction. The breathing dynamics also manifest the frequency-doubling as observed for dynamical fermionization. The width of momentum is much broader and the many-body features for crystallization are showcased in the entire dynamics.

5.4. Correlation dynamics

In this section, we analyze the process of dynamical fermionization and dynamical crystallization utilizing another key measure; one-body Glauber correlation function. The immediate consequence of the different behaviour of the energy as a function of interaction strength (shown later) is the different spreading characteristics of one-body correlation function. The clear distinction is when the spread of one-body correlation is restricted with time, that with dipole-dipole interaction is very fast due to long range tail. In Fig. 4 and Fig. 5, we provide a comprehensive picture of one-body normalized correlation function for contact and dipolar interaction respectively for some selected time. We find, for contact interaction (Fig. 4), at $t = 0$, the correlation is confined around the center with distinct diagonal correlation and vanishing off-diagonal correlation. The two distinct outer humps and two unclear inner humps along the diagonal correlation signify the Tonks-Girardeau

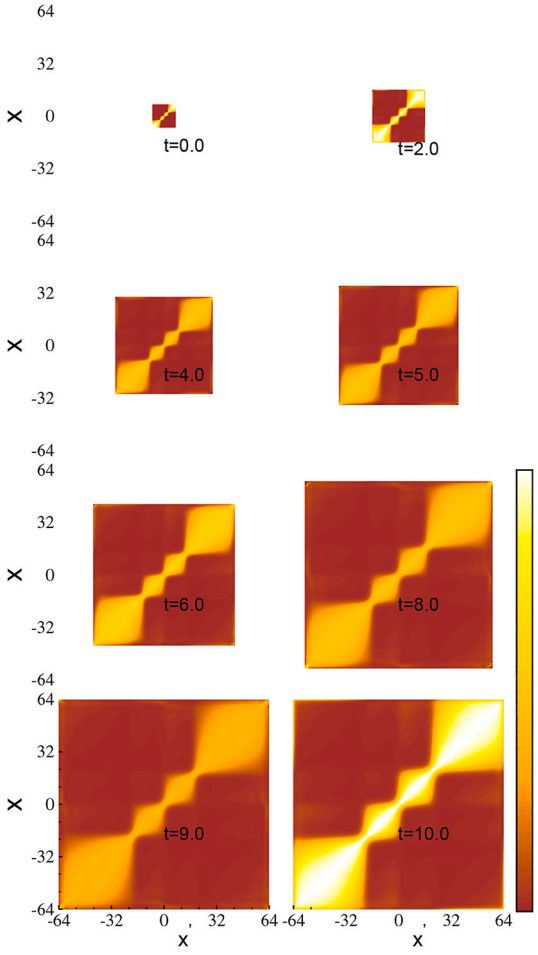

Fig. 5. Dynamics of one-body Glauber correlation function $g^{(1)}(x, x')$ for some selected times on sudden removal of the trap which initially confine four strongly interacting bosons with dipolar interaction in the Tonks-Girardeau limit. All quantities are in dimensionless unit.

gas. On sudden removal of the trap, the correlation spreads with clear development of two inner humps. At $t = 8.0$, when the density of four interacting bosons asymptotically evolve to the density for four noninteracting bosons, dynamical fermionization happens. The corresponding correlation displays four clearly visible but not isolated humps along the diagonal which do not spread further. We infer that the confined spreading of correlation function is the unique signature of dynamical fermionization.

To characterize the dynamical crystallization we plot the one-body correlation function for selected times in Fig. 5. Initially at $t = 0$, the correlation is confined around the center with four well isolated humps characterizing the crystallized state for four interacting dipolar bosons. On sudden expansion, the correlation spreads very fast towards the boundary.

5.5. Distinction of dynamical crystallization from dynamical fermionization

In this section, we will discuss how to distinguish the dynamical crystallization from the dynamical fermionization utilizing evolution of many-body states. In Fig. 6, we plot the energy as a function of interaction strength. It clearly converges to the fermionization limit $E^N_{\lambda\simeq\infty} = \frac{N^2}{2}$ (for the present calculation it is 8.0 for $N = 4$ interacting bosons). The energy for dipolar interaction diverges as a power law. Its immediate consequence is the crystallized bosons have enough interaction energy to overcome the confining potential and spread very fast.

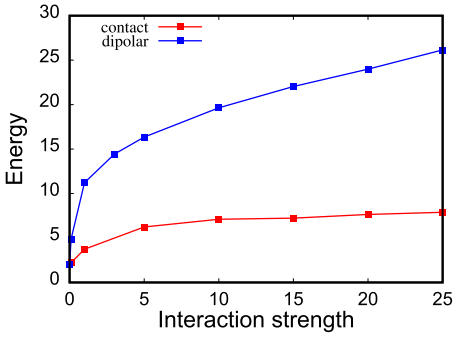

Fig. 6. The energy as a function of interaction strength which converges to the fermionization limit and energy for dipolar interaction which diverges with a power law. All quantities are in dimensionless unit.

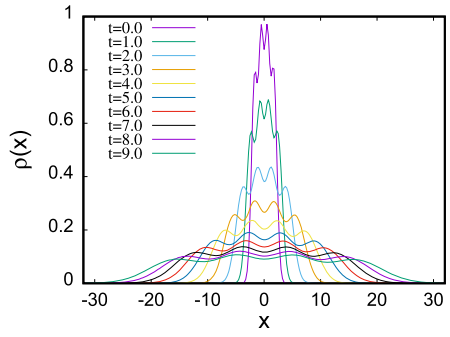

Fig. 7. Dynamics of one-body density for some selected times on sudden removal of the trap which initially confine four strongly interacting bosons with contact interaction in the Tonks-Girardeau limit. All quantities are in dimensionless unit.

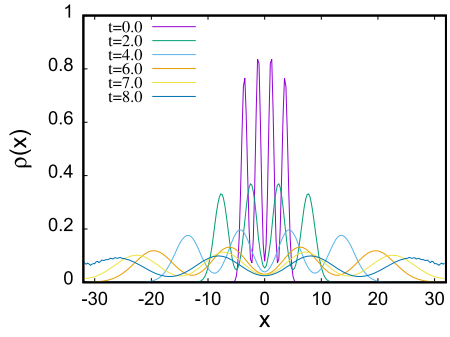

Fig. 8. Dynamics of one-body density for some selected times on sudden removal of the trap which initially confine four strongly interacting bosons with dipolar interaction in the Tonks-Girardeau limit. All quantities are in dimensionless unit.

To visualize the spreading, we plot the one-body density dynamics in Fig. 7 and Fig. 8 for the contact and dipolar interactions respectively in the range $x\epsilon[-32, +32]$. It is clearly seen that for contact interaction in the TG limit, the density spreading exhibits two phenomena: i) the two less prominent outermost peaks gradually become of same height as of the two innermost peaks at the time of fermionization. ii) expansion of the whole cloud. Even after attaining the dynamical fermionization, the fermionized bosons can be traced and do not hit the boundary used in the present simulation. Whereas the spreading of crystallized bosons exhibit one phenomenon - the very fast overall spreading of the whole cloud and just after attaining the crystallization, they are lost after heating the boundary. This manifest the effect of long-range tail in the dynamics.

For tracing the fermionization and crystallization, we quantify the spreading of the density by the position of the outermost peak in the density $\rho(x)$ and plot it in Fig. 9. In both cases, spread of density follows

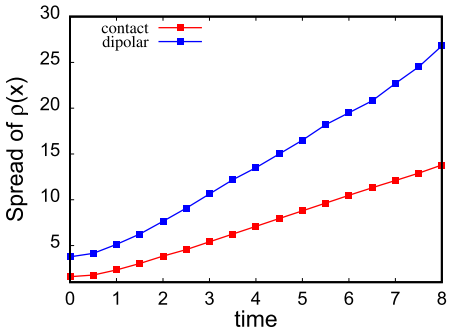

Fig. 9. The spread of the density quantified by the position of the outermost peak in the density $\rho(x)$. The spreading due to dipolar interaction is very fast due to long range repulsive tail. All quantities are in dimensionless unit.

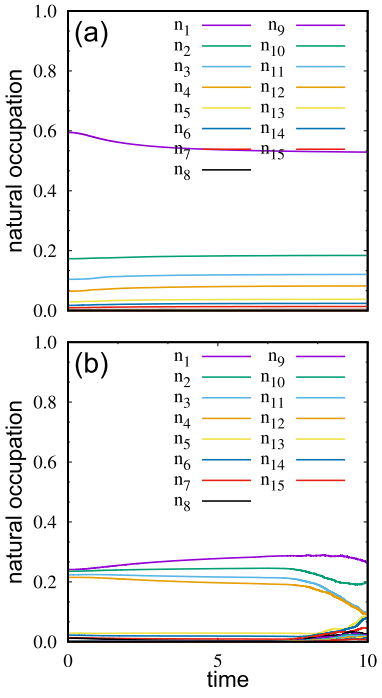

Fig. 10. The eigenvalues of the reduced density matrix, i.e., the natural occupation for 15 orbitals out of 24 orbitals used in the computation. For strongly interacting bosons, the number of significantly contributing orbitals is four which is equal to the number of bosons. For contact interaction, (a), when the fragmentation is depleted, for dipolar interaction it is full-blown 4-fold fragmentation, (b). All quantities are in dimensionless unit.

power law, but for the dipolar interaction the spreading is very fast which causes immediate destruction of crystallized phase. Whereas for contact interaction, the confined spreading causes longer life time of the fermionized phase.

We now turn to analyze the eigenvalues of the reduced one-body density matrix to understand the dynamical fragmentation as presented in Fig. 10. For contact interaction, one natural occupation, n_1, dominates throughout the dynamics, while other three contributing orbitals exhibit the same population during the dynamics. For dipolar interaction, all occupations $\rho_k^{(NO)}$ for $k \leq N$ contribute on an equal footing. The initial full blown 4-fold fragmentation signifies the crystal state which is almost maintained till it hits the wall. The emergence of complete fragmentation is the consequence of long-range dipolar interaction and the emergent depletion is the consequence of contact interaction.

6. Summary and conclusions

We have presented numerically exact results for many-body expansion dynamics and breathing oscillation of dipolar bosons and comparison is made with the fermionization. We solved the N-body Schrödinger equation accurately and from first principles using the multiconfigurational time-dependent Hartree for bosons (MCTDHB). Using the one-body density in real space and momentum space we establish how the fermionization can be distinguished from crystallization. For N-interacting bosons with contact interaction in TG limit, a splitting into an N-fold non isolated pattern forms in the one-body density which is a unique feature of fermionization. Whereas for N-strongly interacting dipolar bosons crystallization is demonstrated by the isolated N-fold pattern. This complete isolation is the consequence of the formation of Mott-insulator like many-body state where lattice potential can be substituted by the long-ranged dipolar interaction and the interparticle interaction stands as a lattice constant. On sudden removal of the trap, the dynamical crystallization is compared with dynamical fermionization and the effect of long range interaction is portrayed in the dynamics. Whereas on sudden reduction of the trap, the bosons with contact interaction exhibit with Bose-Fermi oscillation and result to frequency doubling in momentum space. Whereas for strong dipolar bosons, to capture the Bose-Fermi oscillation and frequency doubling, we need to make double the entire range of real space. The effect of long-range tail in the dipolar interaction is well manifested in the correlation dynamics. The clear crystallization feature is observed in the entire dynamics. All these signatures can be measured experimentally utilizing the single-shot absorption imaging. Thus a direct verification of our results can be performed in the recent experimental set ups in quasi one-dimension.

CRediT authorship contribution statement

Barnali Chakrabarti: Writing – original draft, Supervision, Methodology. **Pankaj Kumar Debnath:** Data curation. **Arnaldo Gammal:** Data curation.

Declaration of competing interest

The authors declare that they have no known competing financial interests or personal relationships that could have appeared to influence the work reported in this paper.

Data availability

No data was used for the research described in the article.

Acknowledgements

BC and AG thank Fundação de Amparo à Pesquisa do Estado de São Paulo (FAPESP), grant nr. 2023/06550-4. AG also thanks the funding from Conselho Nacional de Desenvolvimento Científico e Tecnológico (CNPq), grant nr. 306219/2022-0.

References

[1] K. Aikawa, A. Frisch, M. Mark, S. Baier, A. Rietzler, R. Grimm, F. Ferlaino, Bose-Einstein condensation of erbium, Phys. Rev. Lett. 108 (2012) 210401.
[2] S.S. Alam, T. Skaras, L. Yang, H. Pu, Dynamical fermionization in one-dimensional spinor quantum gases, Phys. Rev. Lett. 127 (2021) 023002.
[3] O.E. Alon, A.I. Streltsov, L.S. Cederbaum, Multiconfigurational time-dependent Hartree method for bosons: many-body dynamics of bosonic systems, Phys. Rev. A 77 (2008) 033613.
[4] A.S. Arkhipov, G.E. Astrakharchik, A.V. Belikov, Y.E. Lozovik, Ground-state properties of a one-dimensional system of dipoles, JETP Lett. 82 (2005) 39.
[5] G.E. Astrakharchik, Y.E. Lozovik, Super-Tonks-Girardeau regime in trapped one-dimensional dipolar gases, Phys. Rev. A 77 (2008) 013404.
[6] G.E. Astrakharchik, G. Morigi, G. De Chiara, J. Boronat, Ground state of low-dimensional dipolar gases: linear and zigzag chains, Phys. Rev. A 78 (2008) 063622.

[7] S. Bera, B. Chakrabarti, A. Gammal, M.C. Tsatsos, M.L. Lekala, B. Chatterjee, C. Lévêque, A.U.J. Lode, Sorting fermionization from crystallization in many-boson wavefunctions, Sci. Rep. 9 (2019) 17873.
[8] I. Bloch, J. Dalibard, S. Nascimbene, Quantum simulations with ultracold quantum gases, Nat. Phys. 8 (2012) 267.
[9] I. Bloch, J. Dalibard, W. Zwerger, Many-body physics with ultracold gases, Rev. Mod. Phys. 80 (2008) 885.
[10] F. Böttcher, J.N. Schmidt, J. Hertkorn, K.S.H. Ng, S.D. Graham, M. Guo, T. Langen, T. Pfau, New states of matter with fine-tuned interactions: quantum droplets and dipolar supersolids, Rep. Prog. Phys. 84 (2021) 012403.
[11] B. Chatterjee, A.U.J. Lode, Order parameter and detection for a finite ensemble of crystallized one-dimensional dipolar bosons in optical lattices, Phys. Rev. A 98 (2018) 053624.
[12] L. Chomaz, I. Ferrrier-Barbut, F. Ferlaino, B. Laburthe-Tolra, B.L. Lev, T. Pfau, Dipolar physics: a review of experiments with magnetic quantum gases, Rep. Prog. Phys. 86 (2023) 026401.
[13] F. Deuretzbacher, J.C. Cremon, S.M. Reimann, Ground-state properties of few dipolar bosons in a quasi-one-dimensional harmonic trap, Phys. Rev. A 81 (2010) 063616.
[14] B. Fang, G. Carleo, A. Johnson, I. Bouchoule, Quench-induced breathing mode of one-dimensional Bose gases, Phys. Rev. Lett. 113 (2014) 035301.
[15] D.M. Gangardt, G.V. Shlyapnikov, Stability and phase coherence of trapped 1D Bose gases, Phys. Rev. Lett. 90 (2003) 010401.
[16] M.D. Girardeau, Permutation symmetry of many-particle wave functions, Phys. Rev. 139 (1965) B500.
[17] A. Griesmaier, J. Werner, S. Hensler, J. Stuhler, T. Pfau, Bose-Einstein condensation of chromium, Phys. Rev. Lett. 94 (2005) 160401.
[18] E. Haller, M.J. Mark, R. Hart, J.G. Danzl, L. Reichsöllner, V. Melezhik, P. Schmelcher, H.C. Nägerl, Confinement-induced resonances in low-dimensional quantum systems, Phys. Rev. Lett. 104 (2010) 153203.
[19] E.H. Lieb, Exact analysis of an interacting Bose gas. II. The excitation spectrum, Phys. Rev. 130 (1963) 1616.
[20] E.H. Lieb, W. Liniger, Exact analysis of an interacting Bose gas. I. The general solution and the ground state, Phys. Rev. 130 (1963) 1605.
[21] R. Lin, P. Molignini, L. Papariello, M.C. Tsatsos, C. Leveque, S.E. Weiner, E. Fasshauer, R. Chitra, MCTDH-X: the multiconfigurational time-dependent Hartree method for indistinguishable particles software, Quantum Sci. Technol. 5 (2020) 024004.
[22] A.U.J. Lode, C. Lévêque, L.B. Madsen, A.I. Streltsov, O.E. Alon, Colloquium: multiconfigurational time-dependent Hartree approaches for indistinguishable particles, Rev. Mod. Phys. 92 (2020) 011001.
[23] A.U.J. Lode, M.C. Tsatsos, E. Fasshauer, S.E. Weiner, R. Lin, L. Papariello, P. Molignini, C. Lévêque, M. Büttner, J. Xiang, S. Dutta, Y. Bilinskaya, Mctdh-x: the multiconfigurational time-dependent Hartree method for indistinguishable particles software, http://ultracold.org. (Accessed 14 April 2024).
[24] M. Lu, N.Q. Burdick, S.H. Youn, B.L. Lev, Strongly dipolar Bose-Einstein condensate of dysprosium, Phys. Rev. Lett. 107 (2011) 190401.
[25] A. Minguzzi, D.M. Gangardt, Exact coherent states of a harmonically confined Tonks-Girardeau gas, Phys. Rev. Lett. 94 (2005) 240404.
[26] D. Muth, B. Schmidt, M. Fleischhauer, Fermionization dynamics of a strongly interacting one-dimensional Bose gas after an interaction quench, New J. Phys. 12 (2010) 083065.
[27] O.I. Patu, Dynamical fermionization in a one-dimensional Bose-Fermi mixture, Phys. Rev. A 105 (2022) 063309.
[28] T. Pohl, E. Demler, M.D. Lukin, Dynamical crystallization in the dipole blockade of ultracold atoms, Phys. Rev. Lett. 104 (2010) 043002.
[29] A. Polkovnikov, K. Sengupta, A. Silva, M. Vengalattore, Colloquium: nonequilibrium dynamics of closed interacting quantum systems, Rev. Mod. Phys. 83 (2011) 863.
[30] M. Rigol, A. Muramatsu, Fermionization in an expanding 1D gas of hard-core bosons, Phys. Rev. Lett. 94 (2005) 240403.
[31] R. Roy, B. Chakrabarti, N.D. Chavda, M.L. Lekala, Information theoretic measures for interacting bosons in optical lattice, Phys. Rev. E 107 (2023) 024119.
[32] R. Roy, B. Chakrabarti, A. Gammal, Out of equilibrium many-body expansion dynamics of strongly interacting bosons, SciPost Phys. Core 6 (2023) 073.
[33] R. Roy, A. Gammal, M.C. Tsatsos, B. Chatterjee, B. Chakrabarti, A.U.J. Lode, Phases, many-body entropy measures, and coherence of interacting bosons in optical lattices, Phys. Rev. A 97 (2018) 043625.
[34] R. Roy, C. Lévêque, A.U.J. Lode, A. Gammal, B. Chakrabarti, Fidelity and entropy production in quench dynamics of interacting bosons in an optical lattice, Quantum Rep. 1 (2019) 304–316.
[35] K. Sakmann, A.I. Streltsov, O.E. Alon, L.S. Cederbaum, Reduced density matrices and coherence of trapped interacting bosons, Phys. Rev. A 78 (2008) 023615.
[36] P. Schauß, J. Zeiher, T. Fukuhara, S. Hild, M. Cheneau, T. Macrì, T. Pohl, I. Bloch, C. Gross, Crystallization in Ising quantum magnets, Science 347 (2015) 1455.
[37] S. Sinha, L. Santos, Cold dipolar gases in quasi-one-dimensional geometries, Phys. Rev. Lett. 99 (2007) 140406.
[38] A.I. Streltsov, O.E. Alon, L.S. Cederbaum, Role of excited states in the splitting of a trapped interacting Bose-Einstein condensate by a time-dependent barrier, Phys. Rev. Lett. 99 (2007) 030402.
[39] J.M. Wilson, N. Malvania, Y. Le, Y. Zhang, M. Rigol, D.S. Weiss, Observation of dynamical fermionization, Science 367 (2020) 1461.
[40] V.I. Yukalov, M.D. Girardeau, Fermi-Bose mapping for one-dimensional Bose gases, Laser Phys. Lett. 2 (2005) 375.
[41] K.L. Zhang, Z. Song, Dynamic crystallization in a quantum Ising chain, Phys. Rev. A 102 (2020) 022211.
[42] S. Zöllner, Ground states of dipolar gases in quasi-one-dimensional ring traps, Phys. Rev. A 84 (2011) 063619.
[43] S. Zöllner, G.M. Bruun, C.J. Pethick, S.M. Reimann, Bosonic and fermionic dipoles on a ring, Phys. Rev. Lett. 107 (2011) 035301.